Large Variations in $^{13}C^{\alpha}$ Chemical Shift Anisotropy in Proteins Correlate with Secondary Structure

Nico Tjandra[†] and Ad Bax*,[‡]

*Laboratory of Biophysical Chemistry
National Heart, Lung, and Blood Institute
Laboratory of Chemical Physics
National Institute of Diabetes and Digestive
and Kidney Diseases
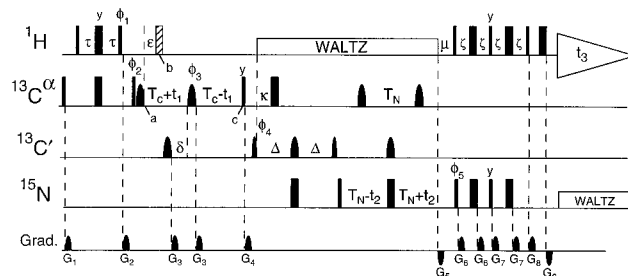National Institutes of Health
Bethesda, Maryland 20892-0520*

In recent years, there has been a renewed interest in the relation between protein structure and chemical shift.[1–8] Most clear-cut has been the correlation between the deviation of $^{13}C^{\alpha}$ chemical shifts from their random coil values (so-called secondary shifts) and the polypeptide backbone angles, ϕ and ψ.[3] Characteristic downfield secondary shifts of ~3 ppm in α-helices and small (~1 ppm) upfield shifts in β-sheet have greatly facilitated the identification of secondary structure.[3,4] The root-mean-square agreement between $^{13}C^{\alpha}$ chemical shifts in the 213-residue protein cutinase and values predicted on the basis of its 1.25-Å crystal structure was only 0.95 ppm.[9] Isotropic shifts only report on the average shielding along three orthogonal axis, and frequently small changes in isotropic shift correspond to much larger changes in chemical shift anisotropy.[10,11] In this case, *ab initio* calculations are expected to be particularly useful at correlating changes in the shielding tensor with structure. Here, we show that quantitative information on the $^{13}C^{\alpha}$ CSA is readily obtained from relatively simple 2D and 3D triple resonance solution state NMR experiments. Results confirm that also for $^{13}C^{\alpha}$, small variations in isotropic chemical shift are accompanied by much larger changes in the CSA tensor.

Relaxation interference (cross correlation)[12] between the $^{13}C-{}^{1}H^{\alpha}$ and $^{13}C^{\alpha}$ CSA interactions results in different transverse relaxation rates, $\lambda \pm \eta$, of the two $^{13}C^{\alpha}-\{^{1}H^{\alpha}\}$ doublet components.[13] The cross-correlation component, η, is given by[10,11,13]

$$\eta = 2\alpha d\{4J(0) + 3J(\omega_C)\} \tag{1}$$

where $J(\omega)$ is the spectral density for dipolar-CSA cross correlation; $d = \gamma_H^2\gamma_C^2h^2/(80\pi^2 r_{HN}^6)$, $\alpha = -4\pi/3B_o(\sigma_{par} - \sigma_{orth})r_{CH}^3/(h\gamma_H)$, and r_{CH} is the $^{13}C-{}^{1}H$ internuclear distance, assumed to be 1.09 Å; σ_{par} is the shielding in the direction

---
† Laboratory of Biophysical Chemistry.
* Laboratory of Chemical Physics.
(1) Ando, I.; Saito, H.; Tabeta, R.; Shoji, A.; Ozaki, T. *Macromolecules* **1984,** *17,* 457–461.
(2) Saito, H. *Magn. Reson. Chem.* **1986,** *24,* 835–852.
(3) Spera, S.; Bax, A. *J. Am. Chem. Soc.* **1991,** *113,* 5490–5492.
(4) Wishart, D. S.; Sykes, B. D.; Richards, F. M. *J. Mol. Biol.* **1991,** *222,* 311–333.
(5) de Dios, A. C.; Pearson, J. G.; Oldfield, E. *Science* **1993,** *260,* 1491–1496.
(6) Pearson, J. G.; Oldfield, E.; Lee, F. S.; Warshel, A. *J. Am. Chem. Soc.* **1993,** *115,* 6851–6862.
(7) Szilagyi, L. *Prog. Nucl. Magn. Reson. Spectrosc.* **1995,** *27,* 325–443.
(8) Heller, J.; Laws, D. D.; Tomaselli, M.; King, D. S.; Wemmer, D. E.; Pines, A.; Havlin, R. H.; Oldfield, E. *J. Am. Chem. Soc.* In press.
(9) Prompers, J. J.; Groenewegen, A.; van Schaik, R. C.; Pepermans, H. A. M.; Hilbers, C. W. *Protein Sci.* In press.
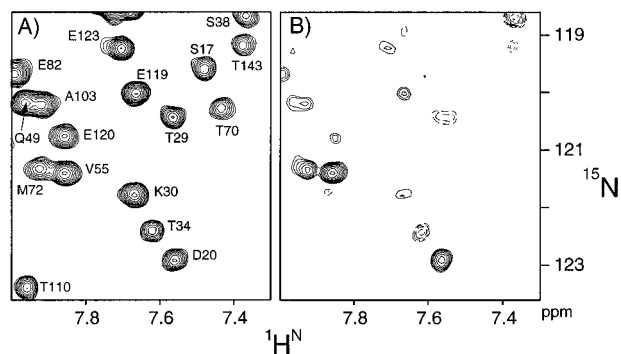(10) Tjandra, N.; Szabo, A.; Bax, A. *J. Am. Chem. Soc.* **1996,** *118,* 6986–6991.
(11) Tjandra, N.; Bax, A. *J. Am. Chem. Soc.* In press.
(12) Werbelow, L. G. *Encyclopedia of Nuclear Magnetic Resonance*; Grant, D. M., Harris, R. K., Editors-in-Chief; Wiley: London, 1996; Vol. 6, pp 4072–4078.
(13) Goldman, M. *J. Magn. Reson.* **1984,** *60,* 437–452.

Figure 1. Pulse schemes for quantitative measurement of cross correlation between $^{13}C^{\alpha}$ CSA and $^{13}C^{\alpha}-{}^{1}H^{\alpha}$ dipolar coupling. The experiment is carried out as either a 2D or a 3D experiment. For the 2D case, one spectrum is recorded with the shaded ^{1}H 180° pulse (A) and one without (B). All resonances observed with scheme B result from cross-correlation during the period $2T_C$; signals observed in scheme A result from regular, INEPT-type magnetization transfer. Narrow and wide pulses correspond to flip angles of 90 and 180°, respectively. Pulses following the WALTZ ^{1}H decoupling yield gradient-enhanced $^{15}N \rightarrow {}^{1}H^{N}$ magnetization transfer.[17] Shaped $^{13}C^{\alpha}$ pulses are of the hyperbolic secant type, with a squareness level of 3, and durations of 500 μs at 151 MHz ^{13}C frequency. The first shaped $^{13}C^{\alpha}$ pulse (time *a*) compensates for phase errors introduced by the second shaped $^{13}C^{\alpha}$ 180° pulse.[18] $^{13}C'$ pulses have the shape of the center lobe of a (sin $x)/x$ function, and durations of 180 μs. The radio-frequency phase of all pulses is *x*, unless indicated. Delay durations: $\tau \approx 1.4$ ms; $\zeta = 2.67$ ms; $T_C = 14$ ms; $T_N = 15$ ms; $\delta = 5.5$ ms; $\Delta = 13$ ms; $\kappa = 4.6$ ms; $\mu = 5.35$ ms. Phase cycling: $\phi_1 = y,-y$; $\phi_2 = y$ (scheme A); $\phi_2 = x$ (scheme B); $\phi_3 = 2(x),2(y)$; $\phi_4 = 4(x),4(-x)$; Rec. $= x,2(-x),x,-x,2(x),-x$. For the 2D experiment, t_1 is kept at zero and Rance-Kay t_2 quadrature detection is used, alternating ϕ_5 between *x* and *y* in concert with the polarity of gradient G_5.[17] For the 3D experiment, the shaded ^{1}H 180° pulse is not applied, the phase cycling of scheme A is used, and t_1 quadrature is obtained by States-TPPI on ϕ_2. All gradients are sine-bell shaped, with 25 G/cm (10 G/cm for $G_{5,8,9}$) at their center. Durations: $G_{1,2,3,4,5,6,7,8,9} = 4, 2, 1, 2.1, 2.705, 1.2, 1.1, 0.2, 0.075$ ms, with respective gradient axes: *xy, xy, xz, yz, z, x, y, z, z.*

parallel to the C–H bond, and σ_{orth} is the average shielding orthogonal to this bond. Note that $\sigma_{par} - \sigma_{orth} = {}^3/2(\sigma_{par} - \sigma_{iso})$, where σ_{iso} is the isotropic shielding. Fully analogous to experiments recently described for measurement of amide proton CSA,[11] η can be measured directly from the ratio, $e^{-2\eta T}$, of the intensities of the two $^{13}C-\{^{1}H^{\alpha}\}$ doublet components after a constant-time evolution period of duration T. Alternatively, the differential relaxation of the two $^{13}C-\{^{1}H^{\alpha}\}$ doublet components partially converts antiphase C_yH_z into in-phase C_y magnetization.[10] The value of η can then be derived from the relative ratio of C_yH_z and C_y.[10] The two methods are clearly very similar to one another and can be performed with nearly identical pulse schemes (Figure 1).

The relative intensities of the two $^{13}C^{\alpha}-\{^{1}H^{\alpha}\}$ doublet componets are measured with the 3D (HA)CA(CO)NH experiment of Figure 1. Magnetization is transferred from $^{1}H^{\alpha}$ to $^{13}C^{\alpha}$ (time point *a*) and subsequently evolves for a constant-time evolution period of length $2T_C \approx 1/J_{C\alpha C\beta} \approx 28$ ms. The shaded 180° ^{1}H decoupling pulse (time *b*) is not applied, and the spectrum will result in an antiphase $^{13}C^{\alpha}-\{^{1}H^{\alpha}\}$ doublet in the F_1 dimension of the 3D spectrum. The relative intensity of two doublet components equals $e^{-4\eta T_C}$. The spectral density, $J(0)$, is approximated most easily on the basis of ^{15}N relaxation measurements,[11,14] assuming that internal motions for the $^{13}C^{\alpha}-{}^{1}H^{\alpha}$ vector are of similar rate and magnitude as those for the backbone N–H. As $J(0) \gg J(\omega_C)$, even errors by as much as 50% in $J(\omega_C)$ would have little effect on deriving $\sigma_{par} - \sigma_{orth}$ from η.

---
(14) Tjandra, N.; Feller, S. E.; Pastor, R. W.; Bax, A. *J. Am. Chem. Soc.* **1995,** *117,* 12562–12566.

Figure 2. Small sections of (A) the reference and (B) the $^{13}C^\alpha$ CSA/$^{13}C^\alpha$–$^1H^\alpha$ dipolar coupling cross correlation (HCACO)NH spectra of the calmodulin/M13 complex. Labels correspond to the $^{13}C^\alpha$ preceding the amide whose resonances are observed in the spectrum. The total measuring time was 1.4 h for part A and 8.5 h for part B.

An alternative, 2D experiment uses the same pulse scheme of Figure 1, but t_1 is kept at zero, and only t_2 is incremented in the usual fashion. Magnetization again originates on H^α and is transferred to $^{13}C^\alpha$ at time a. In a reference experiment (A), the dashed 180° $^1H^\alpha$ pulse is applied a time $\epsilon = 1/(4^1J_{C\alpha H\alpha})$ later, causing $C^\alpha_x H^\alpha_z$ terms to refocus at time c (and dephase with respect to $^{13}C'$), resulting in $C^\alpha_x C'_z$. In a second experiment (B), the 180° $^1H^\alpha$ pulse is not applied (and ϕ_2 is changed by 90°), and only the term resulting from cross correlation ($C^\alpha_y H^\alpha_z \rightarrow C^\alpha_y \rightarrow C^\alpha_x C'_z$) can be transferred to $^{13}C'$, and subsequently to the amide of the next residue.[15] The relative intensity observed in spectra B and A equals[10]

$$I_B/I_A = \tanh(4T_C\eta) \qquad (2)$$

Both experiments have been applied to samples of 1.5 mM U–^{13}C/^{15}N ubiquitin, pH 4.3, 13.6 °C, and to a 1.5 mM complex of U–^{13}C/^{15}N calmodulin (CaM) and a 26-residue unlabeled peptide fragment (M13) of skeletal muscle myosin light chain kinase, pH 6.8, 100 mM KCl, 35 °C.

Figure 2 shows a small region of the calmodulin reference spectrum and the corresponding region of the cross-correlation (HACACO)NH spectrum. The cross-correlation spectrum is plotted at a 3.6-fold lower contour level (after correcting for the difference in the number of scans used for recording the two spectra). Intensities in the cross correlation spectrum for residues in α-helices are very weak, or negative (dashed contours) for Thr and Ser residues, reflecting small or negative values of $\sigma_{orth} - \sigma_{par}$. Residues Asp[20] and Val[55], which follow helices I and III, respectively, have ϕ and ψ angles well outside

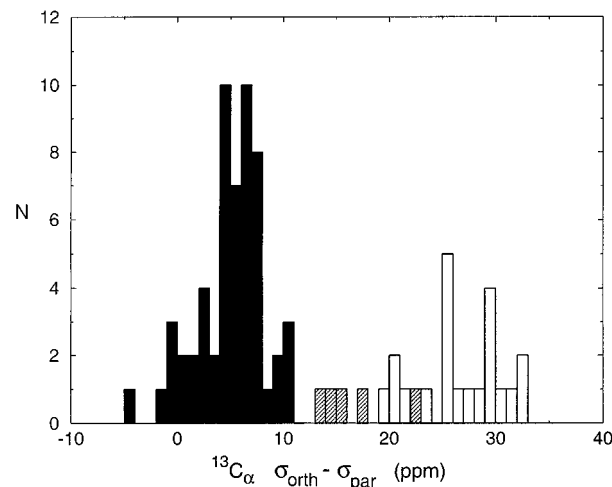(15) Grzesiek, S.; Bax, A. *J. Biomol. NMR* **1993**, *3*, 185–204.
(16) Koradi, R.; Billeter, M.; Wüthrich, K. *J. Mol. Graphics* **1996**, *14*, 52–55.
(17) Kay, L. E.; Keifer, P.; Saarinen, T. *J. Am. Chem. Soc.* **1992**, *114*, 10663–10665.
(18) Conolly, S.; Nishimura, D.; Macovski, A. *Magn. Reson. Med.* **1993**, *18*, 28–38.
(19) Vijay-Kumar, S.; Bugg, C. E.; Cook, W. J. *J. Mol. Biol.* **1987**, *194*, 531–544.
(20) Meador, W. E.; Means, A. R.; Quiocho, F. A. *Science* **1992**, *257*, 1251–1255.

Figure 3. Histogram of $^{13}C^\alpha$ $\sigma_{orth} - \sigma_{par}$ values measured for calmodulin and ubiquitin residues in α-helical (solid) and β-sheet (open) secondary structure, as determined by the program MOLMOL.[16] Hashed bars correspond to five residues identified by MOLMOL as α-helical, but with backbone dihedral angles[19,20] well outside the α-helical range. Thr and Ser residues are not included.

the α-helical range and exhibit intense resonances in the cross-correlation spectrum, reflecting large, positive values of $\sigma_{orth} - \sigma_{par}$.

Analysis of the complete set of $\sigma_{orth} - \sigma_{par}$ values (172 residues, Supporting Information) obained for ubiquitin and for the CaM/M13 complex confirms that $\sigma_{orth} - \sigma_{par}$ is strongly correlated with secondary structure (Figure 3). In α-helices, $\sigma_{orth} - \sigma_{par} = 6.1 \pm 4.9$ ppm, whereas in a β-sheet $\sigma_{orth} - \sigma_{par} = 27.1 \pm 4.3$ ppm. Five α-helical residues with small or negative secondary $^{13}C^\alpha$ chemical shifts (<2 ppm), have $\sigma_{orth} - \sigma_{par}$ values intermediate between α-helix and β-sheet (shaded in Figure 3). All five residues are located at the C-termini of α-helices.

Figure 3 does not include Ser and Thr residues, which have $\sigma_{orth} - \sigma_{par}$ values similar to those of other residues when located in a β-sheet, but significantly negative values in α-helices (Supporting information). Clearly, the $\sigma_{orth} - \sigma_{par}$ values are influenced by the nature of the amino acid side chain and, to a lesser extent, also by the conformation of the side chain.

Our results indicate that large variations in the $^{13}C^\alpha$ CSA are correlated with backbone conformation. This opens exciting new opportunities for determining the exquisitely sensitive relation between chemical shift and protein structure and, ultimately, to increase the accuracy of protein structures determined by NMR.

Supporting Information Available: One table with ubiquitin $^{13}C^\alpha$ $\sigma_{orth} - \sigma_{par}$ values and one table with calmodulin $^{13}C^\alpha$ $\sigma_{orth} - \sigma_{par}$ values, measured with the two methods described in the text; one figure showing 1D cross sections through the 3D spectrum (6 pages). See any current masthead page for ordering and Internet access instructions.